LBL--28335

DE90 009204

Permeability and Dispersivity of Variable-Aperture Fracture Systems

Y. W. Tsang and C. F. Tsang

Earth Sciences Division
Lawrence Berkeley Laboratory
University of California
Berkeley, California 94720

January 1990

This work was supported by the Director, Office of Energy Research, Office of Basic Energy Sciences, Engineering and Geosciences Division, and by the Director, Office of Civilian Radioactive Waste Management, Office of Facilities Siting and Development, Siting and Facilities Technology Division, of the U.S. Department of Energy under Contract No. DE-AC03-76SF00098.

PERMEABILITY AND DISPERSIVITY OF VARIABLE-APERTURE FRACTURE SYSTEMS

Y. W. TSANG and C. F. TSANG
Earth Sciences Division
Lawrence Berkeley Laboratory
University of California
Berkeley, California 94720
(415) 486-5782

ABSTRACT

A number of recent experiments have pointed out the need of including the effects of aperture variation within each fracture in predicting flow and transport properties of fractured media. This paper introduces a new approach in which medium properties, such as the permeability to flow and dispersivity in tracer transport, are correlated to only three statistical parameters describing the fracture aperture probability distribution and the aperture spatial correlation. We demonstrate how saturated permeability and relative permeabilities for flow, as well as dispersion for solute transport in fractures may be calculated. We are in the process of examining the applicability of these concepts to field problems. Results from the evaluation and analysis of the recent Stripa-3D field data are presented.

INTRODUCTION

Recent interest in site characterization and performance assessment of geological formations for the design and construction of nuclear waste repositories has motivated many studies of fluid flow and tracer transport in fractured rocks. For quite a number of years, numerical modeling of fluid flow in the fractured medium was based on the assumption that each fracture may be idealized as a pair of parallel plates separated by a constant distance which represents the aperture of the fracture. Recent work[1-6] have begun to take into account the fact that the apertures in a real fracture takes on a range of values. The wide range of aperture values in a single fracture gives rise to a heterogeneous 2D system with the result that the fluid flow is very non-uniform, and that the majority of flow concentrates in a few preferred paths of least flow resistance. This is the phenomenon of flow channeling, which has been increasingly observed in the field[7-9]. In the presence of flow channeling, the conventional methods of analyzing fluid flow and tracer transport is generally not suitable since they have been formulated for relatively uniform flow in porous media. Our work has been in the development of a new approach to characterize flow and tracer transport in a system of realistic fractures with variable apertures.

Our approach is to construct a conceptual model where the medium properties such as permeability to flow and dispersion of tracer transport may be correlated to only a few statistical parameters of the fracture geometry. In the next section we shall describe our conceptual model of a variable-aperture fracture and the associated characterizing parameters, based on which flow and transport properties of the fracture will be calculated. In the field, the flow and transport properties are best described by parameters such as permeability and dispersivity. Furthermore, in the case of multiphase flow in partially saturated fractures where both air and water occupy the fracture void space, relative permeability curves are needed in addition to the absolute permeability of the medium to describe the flow system. In the following, we shall briefly summarize our work in the study of permeability of the saturated fracture, relative permeabilities of air and water in an unsaturated fracture, as well as the solute dispersivity. We shall conclude our paper with an application of the concepts developed from our theoretical studies to the evaluation and analysis of a set of tracer transport field data in fractured rocks.

DESCRIPTION OF A VARIABLE-APERTURE FRACTURE

Instead of the parallel plate idealization of a fracture, a more realistic representation of a fracture with a range of apertures is adopted by defining a statistical probability distribution function for the aperture values. That the aperture values of laboratory core samples usually follow a skewed distribution well approximated by a lognormal distribution have been shown by a number of researchers[10-11]. The lognormal distribution of apertures b for $b \geq 0$ is given by:

$$n(b)\,db = \frac{1}{\sqrt{2\pi\sigma^2}} \exp\left[\frac{-(\log b - \log b_o)^2}{2\sigma^2}\right] \frac{1}{(\ln 10)\, b}\, db \quad (1)$$

and defined by two parameters: the mean, $(\log b_o)$, and the standard deviation, σ, of the logarithm of aperture. Note that $(1/b)\,db$ is the differential of $\ln b$; the normalization factor $(\ln 10)=2.30258...$ arises from the definition of the aperture distribution on the base 10 logarithm space. The quantity b_o is the

most probable aperture value and is smaller than the mean aperture $\bar{b}$. Equation 1 is a mathematical description of an open fracture with zero contact area between the upper and lower surfaces of the fracture. In general, rock fractures in-situ are partially closed under stress and have contact areas at which the apertures are zero. Such a partially closed fracture may be represented mathematically[1] by a new distribution obtained from truncating the original n(b) by Δb and translating the remaining plot to the origin. The fractional contact area (ω) of the fracture at each fracture closure Δb is simply

$$\omega = \frac{\int_0^{\Delta b} n(b)db}{\int_0^{\infty} n(b)db} \qquad (2)$$

where n(b) is still the aperture distribution when the fracture surface is in point contact under zero applied normal stress. In Figure 1, truncation of the original n(b) corresponding to fractional contact areas of 15, 25, and 35% are marked.

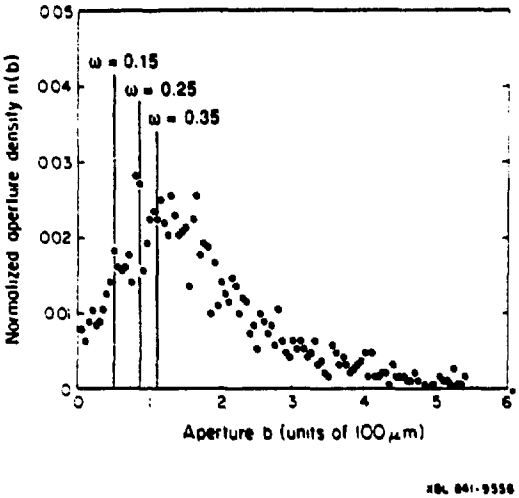

Figure 1. Aperture density distribution n(b) derived from 10 sets of surface roughness profiles of a fracture in granite (data from Gentier[10])

Given the aperture probability density distribution of Equation 1, plus a spatial correlation length parameter, λ, a two-dimensional field of spatially correlated apertures may be generated by geostatistical methods[2]. Many possible spatial distributions or realizations of fracture with variable apertures may be generated by the set of specified parameters: log b_o, σ and λ. Figure 2 shows a discretized version of a particular realization of fracture apertures, with log b_o = 1.7, σ = 0.43 and λ = 0.2 L where L is the linear dimension of the single fracture. The magnitudes of the apertures are indicated by shading, with lighter shading corresponding to larger apertures.

In this paper we shall show results for fractures which have isotropic spatial correlation; studies for systems with different values of λ in orthogonal directions may be found in Tsang and Tsang[5] and Pruess and Tsang[12].

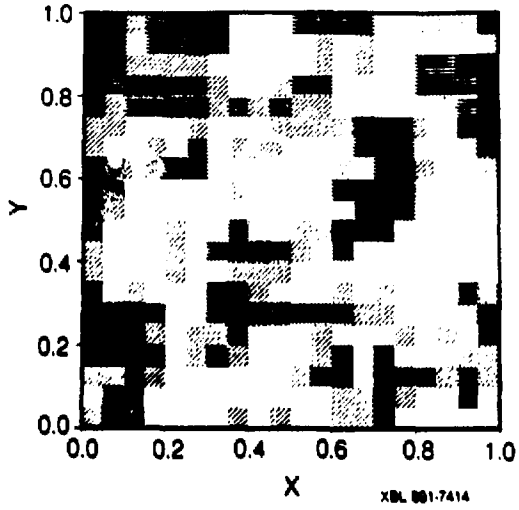

Figure 2. Statistically generated apertures with a spatial correlation length λ of 0.2 L in the plane of a single fracture of linear dimension L. The shadings are given in five levels from small apertures (dark) to large ones (white).

SATURATED PERMEABILITY OF A SINGLE FRACTURE

Assuming that Darcy's law applies locally for a fracture with a range of apertures such as shown in Figure 2, then the local permeability in a water-saturated variable-aperture fracture is proportional to the square of the local aperture and is thus strongly varying in space. Thus the permeability value from a single point pressure flow measurement will be a strong function of the measurement position for a particular realization of fracture aperture distribution. Furthermore, the permeability value from point measurements will also vary strongly for different realizations of fractures characterized by the same parameters log b_o, σ and λ. However, if we consider flow and pressure from a line boundary of the fracture to the line boundary on the opposite side, where the line covers several spatial correlation lengths, it is possible to define a permeability that is independent of statistical realizations. Let us start with a single fracture such as shown in Figure 2 and apply constant pressures, P_1 and P_2, on two opposite sides while maintaining the remaining two sides of the fracture to be no-flow boundaries. The fluid flowrate through the fracture can be calculated by solving a matrix equation relating the pressures at all points in the fracture. The saturated permeability of the fracture, k_{sf}, is then given by the total flowrate from one boundary line to

the other divided by the pressure difference across the fracture. Calculations using many realizations have shown that k_{sf} is defined within a factor of two for specified b_o, σ, and λ, and that it is insensitive to λ if λ is less than 20% or 30% of the size of the 2D flow region. The values of k_{sf}, however, is sensitive to the aperture distribution, i. e., the values of b_o and σ.

We have studied[1] the dependence of the saturated permeability on aperture probability distribution in the context of partially closed fractures with different contact areas ω, as defined in Equation 2. The calculation was carried out for the aperture probability distribution function and three different ω values shown in Figure 1. We may express the results as ratios to the permeability, $\bar{k}$, of a fracture in the parallel-plate approximation, having a constant aperture value equal to the mean aperture of a fracture such as shown in Figure 2. We found that the ratio $k_{sf}/\bar{k}$ is ~ 0.1 when the fracture contact area ω is 15%; 0.04 when ω is 25%, and 0.01 when ω is 35%. Our results, together with confirming experimental observations by Abelin et al.[8], underline the significant role played by small apertures in a variable-aperture fracture on flow permeability, and the pitfall of interpreting permeability measurements in terms of idealized parallel-plate fractures.

RELATIVE PERMEABILITY CURVES FOR UNSATURATED FRACTURES

For unsaturated fractured rocks such as the tuff formation at the proposed repository site at Yucca Mountain, portion of the fracture pore space may be saturated with water and the rest occupied by air or gas phase. The phase occupation depends on water-air capillary pressure given by $P_c = 2\gamma\cos\alpha/b$, where γ is the water-air surface tension, α is the contact angle between the water meniscus and the fracture walls (assumed to be zero in our case), and b is the local fracture aperture value. Water flow is excluded from the air-occupied portion and relative permeability for water depends on connected water-occupied portions in the variable-aperture fracture.

To calculate the relative permeability of water flow, we start with a discretized version of a variable-aperture fracture (Figure 2) and define a cutoff aperture b_c corresponding to a capillary pressure $P_c = 2\gamma/b_c$. All accessible apertures smaller than b_c are occupied with water and all larger apertures with air. The water saturation of the fracture S_w which corresponds to the cutoff capillary pressure P_c is obtained by directly summing the water saturated pore volume. As in the last section on the determination of permeability, a pressure difference is applied across two opposite boundaries of a single fracture and the fluid flow is calculated for a network of water-occupied fracture elements. The steady flowrate obtained will yield the effective water permeability. A similar simulation with the larger b values which are occupied by air will yield the effective air permeability. The above procedure assumes that the pressure gradient is not sizeable so that the two-phase problem in the fracture plane will separate into two separate single-phase problem, which means that the friction between fluid and fracture walls dominates over friction between the two flowing phases. Division of the effective permeability calculated above by the single phase permeability (when all apertures in the fractures are occupied) yields the relative permeability at each saturation S_w. Details of the work may be found in Pruess and Tsang[12].

An example of the relative permeability curves thus calculated for the fracture of Figure 2 is shown in Figure 3. Figure 3 shows an apparently strong interference between the water and air phases with an extremely large immobile air phase saturation of about 84%, and the range of saturation values in which both air and water phases are mobile is virtually non-existent. This arises because a contiguous flow path for air can only be maintained when in addition to all the large apertures some of the small apertures also contain the air phase. In other words, a relatively large air saturation is required before air can flow. Our simulations show that this strong interference between the two phases in two-dimensional flow in fractures persists unless there are long-range spatial correlation among apertures in the direction of flow; then the immobile air phase saturation decreases and there is a range of saturation values in which both air and water phase are flowing. The above results demonstrate the importance of the variable-aperture character of fractures upon air-water flow in unsaturated systems, and more experimental work in the laboratory and in the field is needed to study such systems.

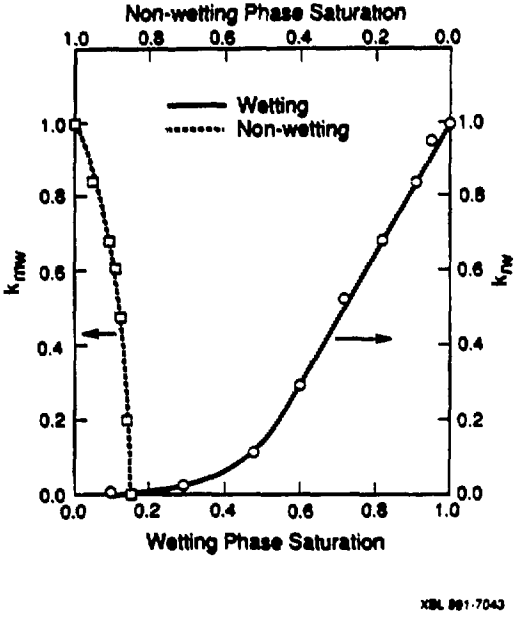

Figure 3. Simulated wetting (water) and nonwetting (air) phase relative permeabilities for the spatial aperture distribution of Figure 2.

TRACER TRANSPORT IN VARIABLE-APERTURE FRACTURE

Tracer residence times and dispersion are important properties which characterize transport in fractured rock masses. In this section we describe the numerical calculation of the tracer breakthrough curves for transport in fractures. Starting with a variable-aperture fracture (e.g. Figure 2) saturated with water, fluid flow from a constant high pressure line boundary to the lower pressure boundary on the opposite side is calculated as before. The local flowrates at different points in the fracture are found to vary over several orders of magnitudes. To display the variation of the large range of flowrates over the entire fracture, the relative volumetric flowrates are plotted in Figure 4 for four realizations of the single fracture where the thickness of the lines varies as the square root of the flowrate. We have carried out this kind of simulation for many realizations of the fracture[2,5]. We found that the flow patterns always display preferred paths of large volumetric flowrates that are formed because of the variation of the apertures within the single fracture plane, and that there is a tendency for all the flow paths with large flowrates to coalesce into "channels" over a width on the order of one spatial correlation length. The spacing between these large flowrate "channels" is also on the order of the spatial correlation length of the fracture apertures.

Starting with distributions of flowrates over a variable-aperture fracture, solute transport phenomena are investigated by tracking the particles advected through the fracture. For each realization as shown in Figure 4, particles are let in at the left hand (higher constant pressure) boundary and collected at the right hand (lower constant pressure) boundary. Plots of the number of particles collected at all the outlets on the right hand boundary as a function of arrival times, i.e., tracer breakthrough curves, are shown in Figure 5. Seven calculated breakthrough curves are shown, four are for the fractures shown in Figure 4 with $\lambda = 0.1$ L, and three are for additional realizations with $\lambda = 0.4$ L. In general, the breakthrough curves of tracer transport in two dimensions through these variable-

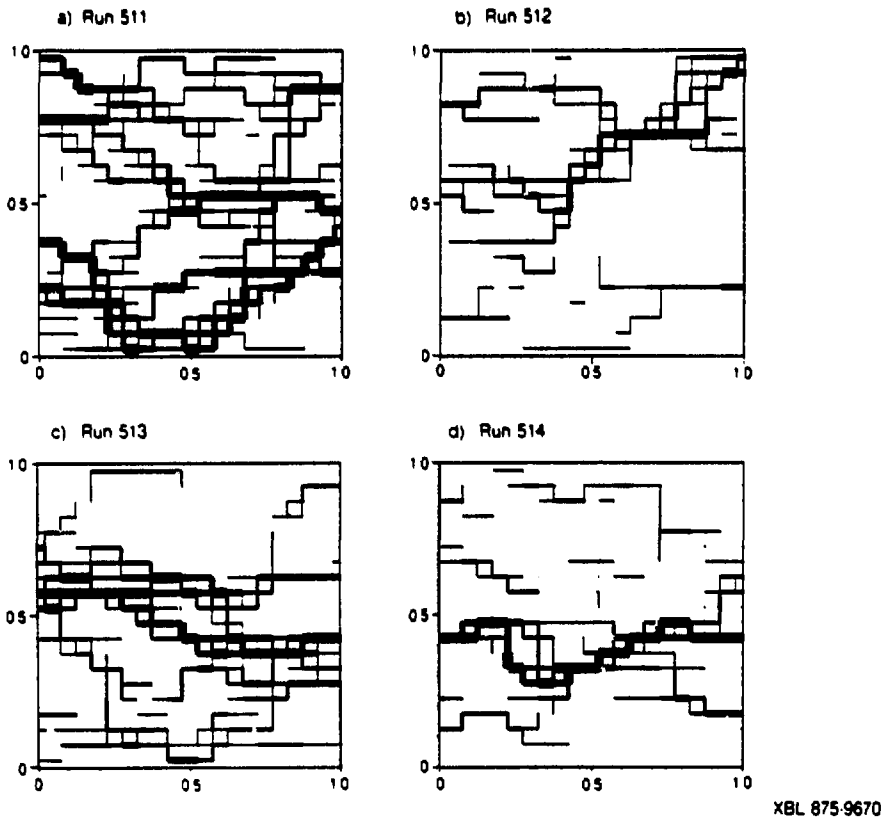

Figure 4. Fluid flowrates for four realizations of the variable-aperture fracture with pressure gradient applied left to right. The thickness of the lines is proportional to the square root of the flowrate for each case.

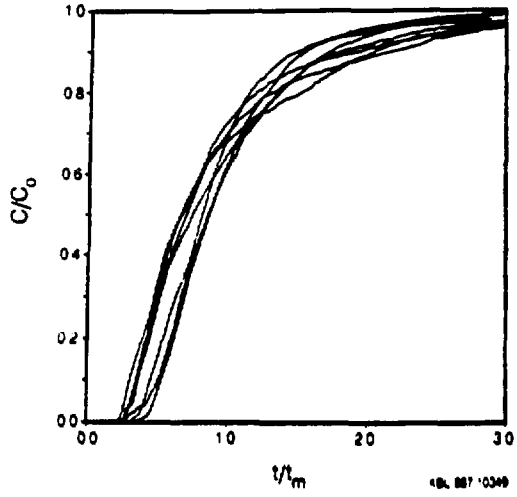

Figure 5. Seven tracer breakthrough curves from particle tracking with time normalized to respective mean residence time, t_m, of all the particles.

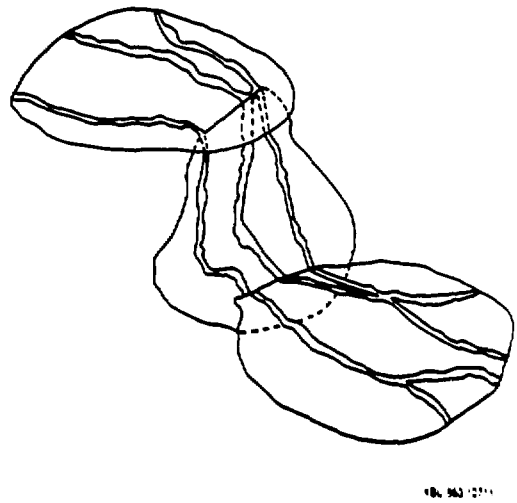

Figure 6. Schematic diagram of channelized flow in three connected variable-aperture fractures.

aperture fractures have a fast rise at early times, since the majority of particles take the fast flow paths. Then, there is a long tail in the breakthrough curve due to a small fraction of particles meandering through the fracture, including in their flowpaths many sections with extremely small volumetric flowrates. In this figure the time axis has been normalized to the respective mean residence time for each case. The fact that these seven curves fall within a narrow band of each other indicates that the dispersion displayed by these breakthrough curves, as measured by the ratio of the difference of 90% and 10% concentration arrival times to the mean arrival time[13], do not vary significantly with different statistical realizations of apertures nor with different correlation lengths. This is because these breakthrough curves involve the residence times of all possible flow paths which originate from the injection line on the left boundary and terminate on the exit line of the right boundary, and both boundaries cover several correlation lengths. Thus the information contained in the breakthrough curves is an average over several correlation lengths, and hence the insensitivity to statistical realizations and correlation length values. On the other hand, these curves are sensitive to the value of standard deviation of log apertures (σ) and Tsang et al.[4] proposed a graphical relationship between σ and dispersion of these fracture tracer breakthrough curves, while the mean residence time may be related to the mean aperture ($\bar{b}$) of the fracture.

Though discussions above refer to tracer transport in one fracture, they can be extended to transport through a few fractures in series as illustrated schematically in Figure 6 for the case of three connected fractures. This picture may be valid when the transport distance covers only a few spacings between conducting fractures. For such a case, the above discussions for one fracture will still apply. In the study of field data (next section), the spacing of conducting fractures versus tracer transport distance is such that the picture (Figure 6) corresponding to a few fractures may still be valid.

APPLICATION TO FIELD DATA

The concepts developed in the theoretical studies described above are used in the understanding of field data. Specifically we have studied the three-year tracer transport field experiment by Neretnieks and coworkers[7] in the Stripa mines, Sweden (Stripa 3D experiment). A drift in Stripa, 75 m long and 4.5 m wide and about 2.5 m high, was used for the experiment. The roof and walls of the drift were covered by over 300 1 × 2 m plastic sheets for collection of water and tracers. Nine different tracers were injected into nine zones of high conductivity in three 75-m vertical boreholes drilled at three locations into the roof. Apparent tracer transport distances from the injection locations to the collection sheets range from 10 to 45 m.

It was found that even though the drift wall appears to be covered with many fractures, only a fraction of the collection sheets received substantial amounts of water. The flowrates to the different collection sheets vary over several orders of magnitude. This is to be expected from the theoretical studies described above (Figures 4 and 6). During the first 30 months, among the nine different tracers only five are found in a small percentage of the collection sheets. The breakthrough curves from the five tracers that arrived at different collection sheets are shown in Figure 7. For each case in this figure we have plotted only the early-time part of the data, since data for later

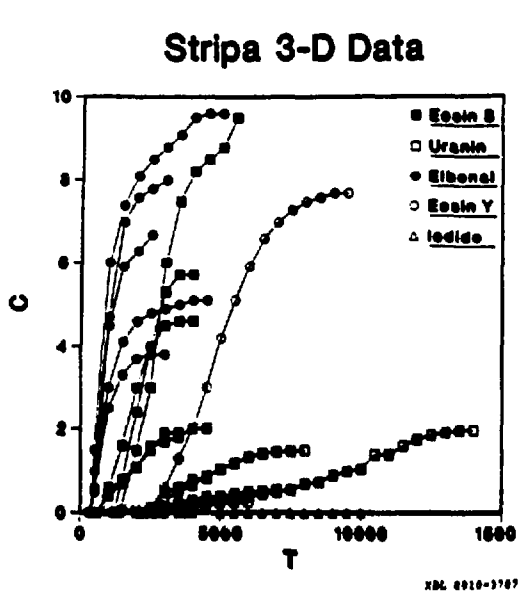

Figure 7. Tracer breakthrough curves from Stripa-3D field experiment. Data are included only up to the first "plateau" beyond which effects of injection flowrate fluctuations become dominant.

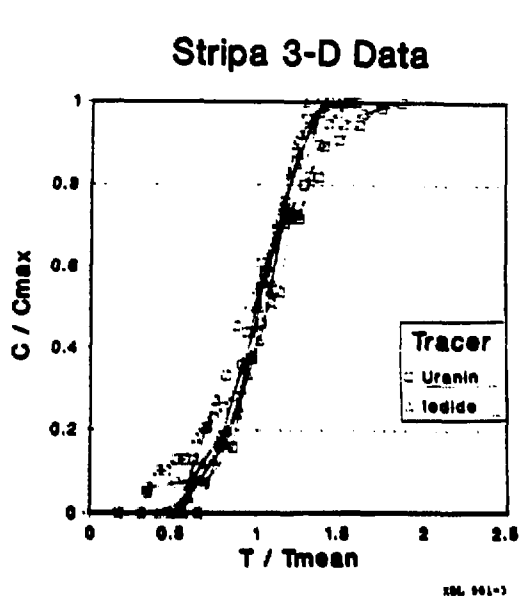

Figure 8. Tracer breakthrough curves for uranin and iodide with apparent transport distance ranging from 20-40 m.

times are very much affected by fluctuations in the experimental tracer injection flowrates. These curves have very different residence times due to different flow paths from channeling, and different maximum concentration because of dilution. However, when we plot them with tracer concentration normalized to each respective maximum value C_{max}, and time t normalized to each respective mean residence time t_m, the curves fall within a small band of each other (Figures 8 and 9). Thus we may argue that the measurements of the transport of different tracers to different collection sheets have sampled different paths in the fractured rock mass characterized by rather similar geometrical fracture parameters. When we analyzed the dispersion from the breakthrough data shown in Figures 8 and 9, we arrive at a dispersion versus distance plot given in Figure 10. Here the dispersion is characterized[13] by the ratio of $(t_{80}-t_{20})$ to t_{50}, with t_x being the time when the tracer concentration reaches x% of C_{max}. A slight decrease of $(t_{80}-t_{20})$ to t_{50} with distance is noted. Further studies are underway to analyze these data and to understand these results.

SUMMARY AND CONCLUSIONS

A number of recent experiments have pointed out the need of including the aperture variability within each fracture in predicting flow and transport properties of fractured media. The paper introduces a new approach to address fracture aperture variations based on a statistical method. Thus only three parameters: the most probable fracture aperture (b_o), standard deviation of apertures (σ), and spatial correlation length (λ) are

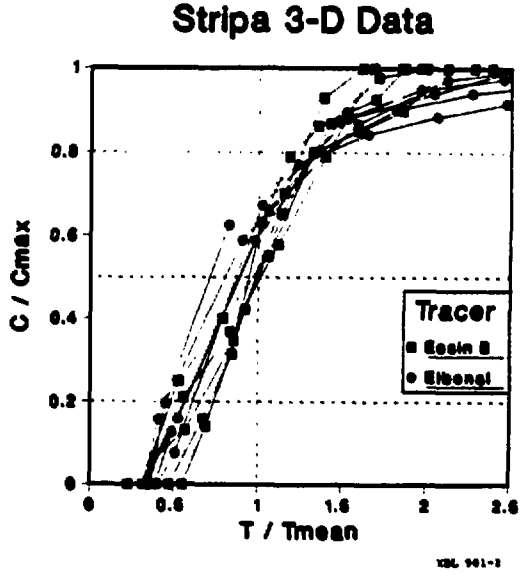

Figure 9. Tracer breakthrough curves for eosin B and elbanol, with apparent transport distance ranging from 10-20 m.

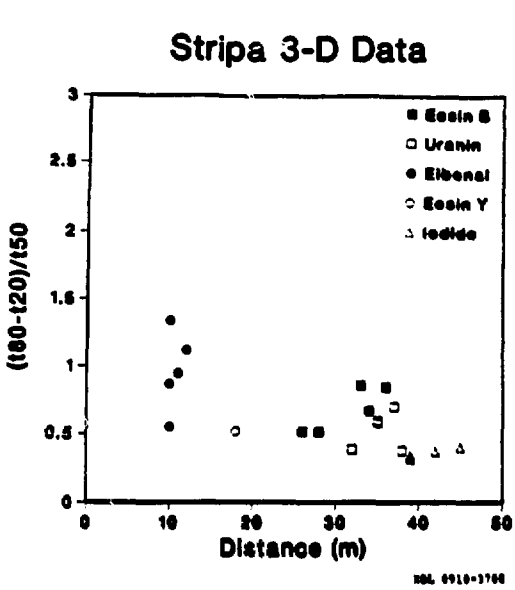

Figure 10. Dispersion as defined by $(t_{80} - t_{20}) / t_{50}$ versus apparent transport distance for all 5 tracers.

used to characterize the fractures. Starting from this concept we demonstrate how saturated permeability, relative permeabilities and solute dispersion of the fractures can be calculated. We are in the process of applying these results and concepts to the understanding of field data.

ACKNOWLEDGMENTS

Careful review and comments from Iraj Javandel and Marcelo Lippmann are gratefully acknowledged. Work is jointly supported by the Director of Office of Energy Research, Office of Basic Energy Sciences, Engineering and Geosciences Division, and by the Director, Office of Civilian Radioactive Waste Management, Office of Facilities Siting and Development, Siting and Facilities Technology Division of the U. S. Department of Energy under Contract No. DE-AC03-76SF00098.

REFERENCES

1. Y. W. TSANG, "The Effect of Tortuosity of Fluid Flow through a Single Fracture," *Water Resour. Res.*, *20*, (9), 1209-1215 (1984).

2. L. MORENO, Y. W. TSANG, C. F. TSANG, F. V. HALE and I. NERETNIEKS, "Flow and Tracer Transport in a Single Fracture: A Stochastic Model and its Relation to some Field Observation," *Water Resour. Res.*, *24*, (12), 2033-2048 (1988).

3. Y. W. TSANG and C. F. TSANG, "Channel Model of Flow through Fractured Media," *Water Resour. Res.*, *23*, (3), 467-479 (1987).

4. Y. W. TSANG, C. F. TSANG, I. NERETNIEKS and L. MORENO, "Flow and Tracer Transport in Fractured Media: A Variable Aperture Channel Model and its Properties," *Water Resour. Res.*, *24*, (12), 2049-2060 (1988).

5. Y. W. TSANG and C. F. TSANG, "Flow Channeling in a Single Fracture as a Two-dimensional Strongly Heterogeneous Permeable Medium," *Water Resour. Res.*, *25*, (9), 2079-2080 (1989).

6. S. R. BROWN, "Fluid Flow through Rock Joints: the Effect of Surface Roughness," *Jour. Geophys. Res.*, 92, (B2), 1337-1347 (1987).

7. I. NERETNIEKS, "Transport in Fractured Rocks," *Proceedings, Memoires of the 17th International Congress of International Association of Hydrologists*, (17), 301-318, International Association of Hydrologists, Tuscon, Ariz. (1985).

8. H. L. ABELIN, L. BERGERSSON, J. GIDLUND, L. MORENO, I. NERETNIEKS, H. WIDEN and J. ANDERSSON, "Results of some Large Scale in Situ Tracer Experiments in a Drift at the Stripa Mine," *Proceedings of International Conference on Fluid Flow in Fractured Rocks*, Atlanta, Georgia, May 16-18 (1988).

9. P. J. BOURKE, "Channeling of Flow through Fractures in Rock," *Proceedings of GEOVAL-87, International Symposium*, Stockholm, Sweden, April 7-9 (1987).

10. S. GENTIER, "Morphologie et Comportment Hydromecanique d'une Fracture Naturelle dans un Granite Sous Contrainte Normale," Doctoral Thesis, U. d'Orleans, France (1986).

11. J. E. GALE, "Comparison of Coupled Fracture Deformation and Fluid Flow Models with Direct Measurements of Fracture Pore Structure and Stress-flow Properties," *Proceedings of 28th U. S. Symposium of Rock Mechanics*, Tuscon, Arizona 29 June-1 July, 1213-1222 (1987).

12. K. PRUESS and Y. W. TSANG, "On Two-phase Relative Permeability and Capillary Pressure of Rough-walled Rock Fractures," accepted for publication in *Water Resour. Res.*, (1990).

13. I. NERETNIEKS, T. ERIKSEN and P. TÄHTINEN, "Tracer Movement in a Single Fissure in Granitic Rock: Some Experimental Results and their Interpretation," *Water Resour. Res.*, *18*, (4), 849-858, (1982).